Refractive Index Sensor for Liquids and Solids Using Dielectric Multilayer Films Deposited on Optical Fiber End Surface

Kyung-Su Kim, Yosuke Mizuno, Masayuki Nakano, Seiichi Onoda, and Kentaro Nakamura, *Member, IEEE*

***Abstract*—We propose and demonstrate a novel fiber-optic refractive index (RI) sensor using dielectric multilayer thin films (DMFs) deposited on an optical fiber end surface, which rejects the incident light with particular wavelength. We experimentally show that the center frequency of the reflected light spectrum changes in proportion to the RI of six kinds of liquids attached to the fiber end. Its coefficient of +0.61 nm/RIU (refractive index unit) agrees well with our simulation results based on characteristic-matrix technique. We also show that this sensor is applicable to the RI measurement of solids.**

***Index Terms*—Bandpass filter, dielectric multilayer film, optical fiber sensor, refractive index sensor.**

I. Introduction

REFRACTIVE-INDEX (RI) sensors are of great significance for wide applications in biochemistry, chemical and environmental analysis, etc [1]–[4]. Many kinds of RI sensors using optical fibers have been developed so far due to their advantages such as compact size, cost efficiency, flexibility in design, remote-sensing capability, multiplexibility, and immunity to electromagnetic interference. Since the simplest fiber-optic RI sensors exploit the power of Fresnel reflection, it is difficult to correctly perform the RI measurement when considerable loss is induced in the fiber. Therefore, various kinds of frequency-domain techniques have been proposed so far. Four of their typical examples are: RI sensors based on (1) fiber Bragg gratings (FBGs), (2) long-period gratings (LPGs), (3) interferometers, and (4) tapered fibers. RI sensors using FBGs [5]–[7] including tilted FBGs (TFBGs) [8]–[10] have high sensitivity, but suffer from low spatial resolution due to their relatively large sensing areas. Besides, we need to etch the cladding to gain access to the evanescent field of the guided mode. LPG-based RI sensors [11]–[13] with high sensitivity have also been developed. Although we need not etch the cladding, they have the same drawbacks as FBG-based RI sensors. On the other hand, many types of RI sensors based on interferometers, including Mach–Zehnder type [14], [15], Michelson type [16], Fabry–Perot type [17], [18], etc. have been implemented, some of which have such advantages as high sensitivity, high spatial resolution, cost efficiency, and simple setup. Furthermore, using tapered fiber ends, Y.-H. Tai *et al.* [19] have recently developed RI sensors with high sensitivity and high spatial resolution. All the fiber-optic RI sensors previously developed, however, have been applied only to the RI measurement of liquids and gases, partly because of their fragility of the sensor heads.

In the meantime, we have recently developed a method to deposit dielectric multilayer thin films (DMFs) on an optical fiber end as an optical bandpass filter (BPF). This structure, called a BPF on a fiber end (BOF) [20], eliminates the incident light with particular wavelength. Since this wavelength depends on temperature and pressure, BOFs have been utilized to develop temperature/pressure sensors with robustness and high spatial resolution [20], [21].

In this letter, we demonstrate that a BOF can be applied to an RI sensor with applicability not only to gases or liquids but also to solids. The center frequency of the reflected light spectrum was found to shift in proportion to the RI of the materials attached to the BOF. Its coefficient was +0.61 nm/RIU, which is in good agreement with our simulation results using characteristic-matrix technique.

II. Principle

A BOF is composed of DMFs deposited on the end face of an optical fiber [20]. The DMFs, typically comprising SiO_2 and TiO_2 layers accumulated by ion-assisted evaporation, form an optical cavity, which serves as a BPF. Thus, the incident light with particular wavelength is selectively eliminated. Fig. 1 shows a scanning electron microscope (SEM) image of the BOF layer structure used in the experiment. It has a Fabry-Perot-type cavity composed of a 925-nm-thick SiO_2 layer. The reflective layers surrounding the cavity, which serve as distributed Bragg reflectors (DBRs), comprise several pairs of $SiO_2(n = 1.46)$ and $TiO_2(n = 2.22)$ layers with the same physical thicknesses of 215 nm (Note that, in general, not physical but optical thickness is designed to be the same). The TiO_2 top layer protecting

Manuscript received May 23, 2011; revised June 30, 2011; accepted July 16, 2011. Date of publication August 15, 2011; date of current version September 23, 2011. This work was supported in part by the "Global Center of Excellence (G-COE) Program" from the Ministry of Education, Culture, Sports, Science and Technology (MEXT), Japan. The work of Y. Mizuno was supported by the Research Fellowships for Young Scientists from the Japan Society for the Promotion of Science (JSPS).

K.-S. Kim, Y. Mizuno, and K. Nakamura are with Precision and Intelligence Laboratory, Tokyo Institute of Technology, Yokohama 226-8503, Japan (e-mail: kskim@sonic.pi.titech.ac.jp; ymizuno@sonic.pi.titech.ac.jp; knakamur@sonic.pi.titech.ac.jp).

M. Nakano and S. Onoda are with the R&D Division, Watanabe, Inc., Saitama 338-0835, Japan (e-mail: nakano@watanabe-mj.co.jp; onoda@watanabe-mj.co.jp).

Color versions of one or more of the figures in this letter are available online at http://ieeexplore.ieee.org.

Digital Object Identifier 10.1109/LPT.2011.2163063

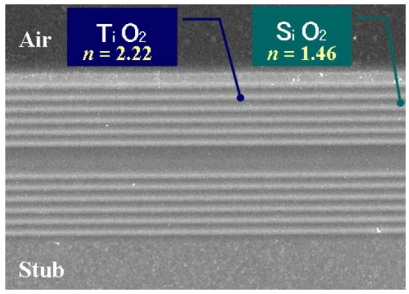

Fig. 1. Layer structure of BOF (SEM image).

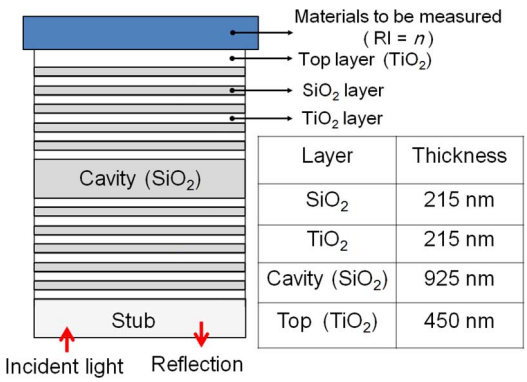

Layer	Thickness
SiO_2	215 nm
TiO_2	215 nm
Cavity (SiO_2)	925 nm
Top (TiO_2)	450 nm

Fig. 2. Simulation model of the BOF structure. The inset table shows the thicknesses of each layer.

the whole structure is 450-nm-thick, which slightly broadens the linewidth of the reflection spectra.

BOFs have been exploited as key components of optical fiber sensors, since its reflection wavelength almost linearly depends on temperature [20] and pressure [21]. This is because the thickness of each layer changes according to temperature and pressure. In this letter, we show that a BOF can be applied also to RI sensing. When materials with different RIs are attached to the BOF, the center wavelength λ_0 shifts depending on the RI. Since λ_0 dependence on RI is almost linear, we can easily derive RI by measuring λ_0. This dependence appears to be caused by the change of Fresnel reflectivity at the interface between the top layer and the materials attached, this behavior should be further clarified in the simulation.

III. Simulation

In order to clarify the RI dependence of the center wavelength λ_0, we performed a numerical simulation based on so-called characteristic-matrix technique [22], [23]. This technique is often used to characterize the optical properties of DMFs, because we need not directly consider the effects of standing waves or integrate multiple reflected signals.

Fig. 2 depicts the BOF model used in the simulation, which was produced based on the SEM image shown in Fig. 1. It includes several pairs of SiO_2/TiO_2 layers and one cavity composed of SiO_2. The materials to be measured are located on the top layer. The thicknesses of each layer are summarized in the inset table in Fig. 2.

Fig. 3(a) represents the simulated RI dependence of the reflection spectra around the center wavelength λ_0. The values

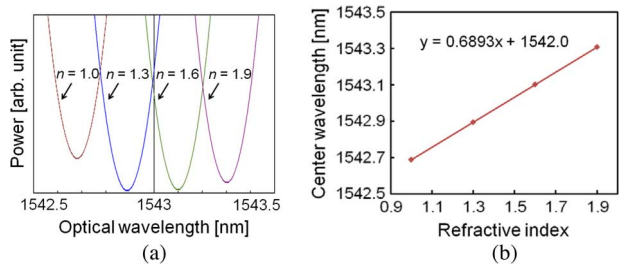

Fig. 3. (a) Simulated RI dependence of the reflected spectrum. The vertical axis is in arbitrary units (b) Center wavelength versus RI.

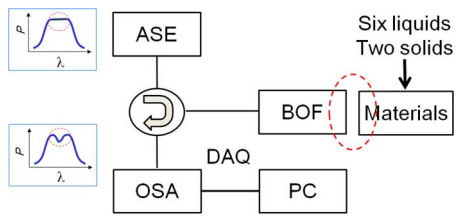

Fig. 4. Experimental setup for the RI measurement using a BOF. ASE" amplified spontaneous emission; DAQ: data acquisition; OSA: optical spectrum analyzer; PC: personal computer.

of RI for the materials were set to 1.0, 1.3, 1.6, and 1.9. From this figure, we can derive the RI dependence of λ_0, as shown in Fig. 3(b). Its slope was almost linear with a coefficient of $+0.6893$ nm/RIU. Thus, we confirmed in the simulation that a BOF can be applied to RI sensing.

IV. Experiments

The experimental setup for measuring RI using a BOF is schematically shown in Fig. 4. Amplified spontaneous emission (ASE) of an erbium-doped fiber (EDF) was used as a light source, and its output was guided to the BOF through an optical circulator. The reflected light from the BOF (reflectivity $\sim$8 dB) was observed with an optical spectrum analyzer (OSA), and the spectral data was transferred to a personal computer (PC) for further processing. We employed air, six kinds of liquids, and two kinds of solids as materials to be measured. The liquids were water $(n \sim 1.33)$, ethanol $(n \sim 1.36)$, salt water (30%) $(n \sim 1.38)$, index-matching oil (I) $(n \sim 1.44)$, matching oil (II) $(n \sim 1.60)$ and matching oil (III) $(n \sim 1.74)$; and the solids were rubber $(n \sim 1.50)$ and plastic $(n \sim 1.65)$.

Fig. 5(a) shows the measured spectra when air and six kinds of liquids were attached to the BOF. It is clear that the spectra change according to the materials with different RI. From Fig. 5(a), the RI dependence of the center wavelength λ_0 can be derived as shown in Fig. 5(b). The measured coefficient of $+0.6115$ nm/RIU was in good agreement with the simulated value of $+0.6893$ nm/RIU. The difference in power between Figs. 3(a) and 5(a) and the discrepancy of the coefficients probably originate from the simulation method where light attenuation in each layer is not taken into consideration.

Then, the experiments were performed in the same manner, when the materials to be measured were solids. Fig. 6 shows the measured spectra when air, rubber, and plastic were attached to the BOF end by hand. The center wavelength λ_0 in the case

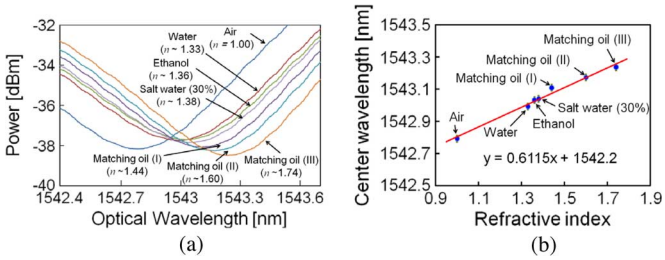

Fig. 5. (a) Reflection spectra with air and six kinds of liquids employed as materials to be measured. (b) Dependence of the center wavelength on RI.

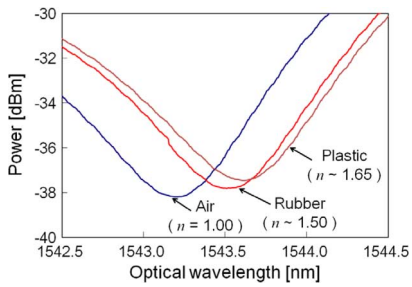

Fig. 6. Reflection spectra with air and two kinds of solids employed as materials to be measured.

of air was longer than that in Fig. 5(a), because the room temperature was slightly higher in Fig. 6 than in Fig. 5(a). From the figure, the RIs of the rubber and the plastic were calculated back to be 1.49 and 1.65, respectively, which agree well with the RIs described in their specification sheets. Thus, we clarified that BOF-based RI sensors can be applied not only to gases or liquids but also to solids. Here, we must bear in mind that it is difficult to apply the BOF sensors to solids with extremely smooth surfaces, such as metals, because induced multiple reflection significantly distorts the reflected spectra.

V. Conclusion

We demonstrated that a BOF sensor with high spatial resolution and robustness is applicable not only to gases or liquids but also to solids. First, its operation was clarified in the simulation using the characteristic-matrix technique. Then, in the experiments with air and six different kinds of liquids, a coefficient of +0.61 nm/RIU was obtained, which agreed well with the simulation result. Furthermore, the RIs of two kinds of solids were also successfully measured.

In order to practically use this RI sensor, a method to compensate the temperature effect must be developed by, for example, fabricating the BOF onto an FBG [24]. The sensitivity also must be improved by employing so-called push-pull technique [20] and using BOFs with different structures. We believe this RI sensor will be of great use in wide range of biochemical, chemical, and engineering applications in future.

References

[1] , F. T. S. Yu and S. Yin, Eds., *Fiber Optic Sensors*. New York: Marcel Dekker, 2002.

[2] Y. J. Rao, "Recent progress in applications of in-fibre Bragg grating sensors," *Opt. Lasers Eng.*, vol. 31, no. 4, pp. 297–324, Apr. 1999.

[3] Y. J. Rao, D. J. Webb, D. A. Jackson, L. Zhang, and I. Bennion, "In fiber Bragg-grating temperature sensor system for medical applications," *J. Lightw. Technol.*, vol. 15, no. 5, pp. 779–785, May 1997.

[4] K. Zhou, X. Chen, L. Zhang, and I. Bennion, "High-sensitivity optical chemsensor based on etched D-fibre Bragg gratings," *Electron. Lett.*, vol. 40, no. 4, pp. 232–234, Feb. 2004.

[5] K. Schroeder, W. Ecke, R. Mueller, R. Willsch, and A. Andreev, "A fibre Bragg grating refractometer," *Meas. Sci. Technol.*, vol. 12, no. 7, pp. 757–764, Jul. 2001.

[6] W. Liang, Y. Huang, Y. Xu, R. K. Lee, and A. Yariv, "Highly sensitive fiber Bragg grating refractive index sensors," *Appl. Phys. Lett.*, vol. 86, no. 15, pp. 151122–151124, Apr. 2005.

[7] A. Iadicicco, A. Cusano, A. Cutolo, R. Bernini, and M. Giordano, "Thinned fiber Bragg gratings as high sensitivity refractive index sensor," *IEEE Photon. Technol. Lett.*, vol. 16, no. 4, pp. 1149–1151, Apr. 2004.

[8] G. Laffont and P. Ferdinand, "Tilted short-period fibre-Bragg-grating—Induced coupling to cladding modes for accurate refractometry," *Meas. Sci. Technol.*, vol. 12, no. 7, pp. 765–770, Jan. 2001.

[9] C. Caucheteur and P. Megret, "Demodulation technique for weakly tilted fiber Bragg grating refractometer," *IEEE Photon. Technol. Lett.*, vol. 17, no. 12, pp. 2703–2705, Dec. 2005.

[10] C. Chan, C. Chen, A. Jafari, A. Laronche, D. J. Thomson, and J. Albert, "Optical fiber refractometer using narrowband cladding-mode resonance shifts," *Appl. Opt.*, vol. 46, no. 7, pp. 1142–1148, Mar. 2007.

[11] V. Bhatia and A. M. Vengsarkar, "Optical fiber long-period grating sensors," *Opt. Lett.*, vol. 21, no. 9, pp. 692–694, May 1996.

[12] D. W. Kim, Y. Zhang, K. L. Cooper, and A. Wang, "In-fiber reflection mode interferometer based on a long-period grating for external refractive-index measurement," *Appl. Opt.*, vol. 44, no. 26, pp. 5368–5373, Sep. 2005.

[13] H. J. Patrick, A. D. Kersey, and F. Bucholtz, "Analysis of the response of long period fiber gratings to external index of refraction," *J. Lightw. Technol.*, vol. 16, no. 9, pp. 1606–1612, Sep. 1998.

[14] Y. Wang, M. Yang, D. N. Wang, S. Liu, and P. Lu, "Fiber in-line Mach–Zehnder interferometer fabricated by femtosecond laser micromachining for refractive index measurement with high sensitivity," *J. Opt. Soc. Amer. B*, vol. 27, no. 3, pp. 370–374, Mar. 2010.

[15] E. M. Dianov, S. A. Vasiliev, A. S. Kurkov, O. I. Medvedkov, and V. N. Protopopov, "In-fiber Mach–Zehnder interferometer based on a pair of long-period gratings," *ECOC'96*, pp. 65–68, Sep. 1996.

[16] Z. Tian, S. S.-H. Yam, J. Barnes, W. Bock, P. Greig, J. M. Fraser, H. P. Loock, and R. D. Oleschuk, "Refractive index sensing with Mach–Zehnder interferometer based on concatenating two single mode fiber tapers," *IEEE Photon. Technol. Lett.*, vol. 20, no. 8, pp. 626–628, Apr. 2008.

[17] Z. Tian, S. S.-H. Yam, and H. P. Loock, "Refractive index sensor based on an abrupt taper Michelson interferometer in a single-mode fiber," *Opt. Lett.*, vol. 33, no. 10, pp. 1105–1107, May 2008.

[18] Z. L. Ran, Y. J. Rao, W. J. Liu, X. Liao, and K. S. Chiang, "Laser-micromachined Fabry–Perot optical fiber tip sensor for high-resolution temperature-independent measurement of refractive index," *Opt. Exp.*, vol. 16, no. 3, pp. 2252–2263, Feb. 2008.

[19] Y. H. Tai and P. K. Wei, "Sensitive liquid refractive index sensors using tapered optical fiber tips," *Opt. Lett.*, vol. 35, no. 7, pp. 944–946, Apr. 2010.

[20] S. Onoda, N. Tsukamoto, M. Ogino, K. Yamashita, O. Yumoto, K. Inoue, and Y. Komatsu, "A proposal of temperature sensing using a thin-film bandpass filter and dual-wavelength push-pull reflectometry," *IEEE Photon. Technol. Lett.*, vol. 20, no. 9, pp. 688–690, May 2008.

[21] Y. Komatsu and S. Onoda, "A novel optical temperature and pressure sensing system," in *Proc. SICE Annual Conf.*, Aug. 2008, pp. 334–337.

[22] R. A. Craig, "Method for analysis of the characteristic matrix in optical systems," *J. Opt. Soc. Amer. A*, vol. 4, no. 6, pp. 1092–1096, Jun. 1987.

[23] I. Wakabayashi and K. Miyauchi, "Design of dielectric multilayer bandpass filters using arbitrary thickness of layers," *Electron. Commun. Jpn.*, vol. 80, no. 1, pp. 46–58, Dec. 1997.

[24] H. J. Patrick, G. M. Williams, A. D. Kersey, J. R. Pedrazzani, and A. M. Vengsarkar, "Hybrid fiber Bragg grating/long period fiber grating sensor for strain/temperature discrimination," *IEEE Photon. Technol. Lett.*, vol. 8, no. 9, pp. 1223–1225, Sep. 1996.